LPCVD homoepitaxy of Si doped β-Ga_2O_3 thin films on (010) and (001) substrates

Subrina Rafique, Md Rezaul Karim, Jared M. Johnson, Jinwoo Hwang, and Hongping Zhao

Citation: Appl. Phys. Lett. **112**, 052104 (2018); doi: 10.1063/1.5017616
View online: https://doi.org/10.1063/1.5017616
View Table of Contents: http://aip.scitation.org/toc/apl/112/5
Published by the American Institute of Physics

LPCVD homoepitaxy of Si doped β-Ga_2O_3 thin films on (010) and (001) substrates

Subrina Rafique,[1,2,a)] Md Rezaul Karim,[1] Jared M. Johnson,[3] Jinwoo Hwang,[3] and Hongping Zhao[1,2,3,b)]
[1]*Department of Electrical and Computer Engineering, The Ohio State University, Columbus, Ohio 43210, USA*
[2]*Department of Electrical Engineering and Computer Science, Case Western Reserve University, Cleveland, Ohio 44106, USA*
[3]*Department of Materials Science and Engineering, The Ohio State University, Columbus, Ohio 43210, USA*

(Received 28 November 2017; accepted 19 January 2018; published online 31 January 2018)

This paper presents the homoepitaxy of Si-doped β-Ga_2O_3 thin films on semi-insulating (010) and (001) Ga_2O_3 substrates via low pressure chemical vapor deposition with a growth rate of ≥ 1 μm/h. Both high resolution scanning transmission electron microscopy and X-ray diffraction measurements demonstrated high crystalline quality homoepitaxial growth of these thin films. Atomic resolution STEM images of the as-grown β-Ga_2O_3 thin films on (010) and (001) substrates show high quality material without extended defects or dislocations. The charge carrier transport properties of the as-grown Si-doped β-Ga_2O_3 thin films were characterized by the temperature dependent Hall measurement using van der Pauw patterns. The room temperature carrier concentrations achieved for the (010) and (001) homoepitaxial thin films were $\sim 1.2 \times 10^{18}$ cm^{-3} and $\sim 9.5 \times 10^{17}$ cm^{-3} with mobilities of ~ 72 cm^2/V s and ~ 42 cm^2/V s, respectively. *Published by AIP Publishing.*
https://doi.org/10.1063/1.5017616

Transparent conducting oxide (TCO) beta gallium oxide (β-Ga_2O_3) is an emerging semiconductor material with an ultrawide room temperature bandgap in the range of $\sim$4.5–4.9 eV and an estimated high breakdown field in the range of $\sim$6–8 MV/cm.[1] It exhibits high transparency in the deep UV and visible wavelength region, which also makes it an attractive candidate for solar blind photodetectors.[2–4] The most promising application of β-Ga_2O_3 lies in the field of high power electronic devices such as Schottky barrier diodes (SBDs)[5–7] and field effect transistors (FETs).[8–10] It is promising to outperform the existing SiC and GaN based electronic device technologies. Moreover, high quality single crystalline β-Ga_2O_3 native substrates can be synthesized by scalable and low cost melt based growth techniques such as floating zone,[11] edge-defined film fed (EFG),[12] and Czochralski[13] methods. This offers a key advantage for β-Ga_2O_3 as it enables homoepitaxial growth of high quality films that are critical for high performance device applications. Particularly, β-Ga2O3 homoepitaxial growth on native substrates allows the deposition of thick films for vertical devices with high breakdown voltage operation, which is difficult to achieve with an active film grown on foreign substrates.

The growth of high quality epitaxial thin films with a reasonable growth rate and controllable doping in a wide range is essential for all the aforementioned applications. The homoepitaxial growth of β-Ga_2O_3 thin films by molecular beam epitaxy (MBE), metal organic vapor phase epitaxy (MOVPE), halide vapor phase epitaxy (HVPE), and low pressure chemical vapor deposition (LPCVD) has been reported previously. The growths were conducted on substrates with different preferred crystal orientations.[14–17] N-type doping of β-Ga_2O_3 thin films to achieve carrier concentrations in the range between 10^{16} and 10^{19} cm^{-3} using Sn and 10^{17}–10^{19} cm^{-3} using Ge in MBE,[18,19] 10^{17}–10^{19} cm^{-3} using Si and Sn in MOVPE,[20,21] 10^{16}–10^{19} cm^{-3} using Si in LPCVD,[22] and 10^{19}–10^{20} cm^{-3} using Si in pulsed laser deposition (PLD)[23] has been reported. When using Sn as an n-type dopant in MOVPE growth, it leaves pronounced memory effects inside the growth chamber. As a result, it is hard to grow a thin film with a low doping concentration after high dopant flow growth. The Sn dopant also forms different complexes and extended defects in the thin films which in turn degrade the material quality.[21] Both MBE and MOVPE growths of β-Ga_2O_3 thin films prefer the (010) orientation of the native substrate.[18,19,21] In the case of MBE, the (010) growth direction is preferred due to the faster growth rate as compared to the film grown on other crystal planes such as (100). The lower adhesion energy of the (100) plane results in the reevaporation of the supplied atoms which in turn lowers the growth rate.[18] There are reports on the homoepitaxial growth of n-type β-Ga_2O_3 thin films on both (100) and (010) native substrates by MOVPE.[20,21] The properties of the thin films grown on (100) substrates were largely affected by the formation of planar defects such as stacking faults and twins.[21] Such defects were formed due to the nucleation of 2D islands with two different orientations rotated by 180° on the (100) plane.[21] The homoepitaxial growth of β-Ga_2O_3 thin films by HVPE has only been reported on the (001) orientation of the native substrate.[16] We have reported unintentional doped (UID) β-Ga_2O_3 thin films growth on the (010) substrate by LPCVD.[17]

In this work, we investigated the LPCVD growth of Si doped n-type β-Ga_2O_3 homoepitaxial thin films on both (010) and (001) Fe doped semi-insulating β-Ga_2O_3 substrates. The growth rates of the LPCVD β-Ga2O3 on both (010) and (001) substrates are demonstrated as ≥ 1 μm/h. The surface morphology and crystal quality of the grown films were characterized by atomic force microscopy (AFM),

a)Email: subrina.rafique@case.edu
b)Author to whom correspondence should be addressed: zhao.2592@osu.edu

X-ray diffraction (XRD) rocking curve, and scanning transmission electron microscopy (STEM), revealing very high crystalline quality. The temperature dependence of the carrier concentration and the electron mobility for the as-grown thin films on both types of substrate orientations were compared and discussed.

The homoepitaxial growth of β-Ga_2O_3 thin films was carried out in a custom-designed tube furnace with a programmable temperature controller and a precise pressure controller. Commercial β-Ga_2O_3 (010) and (001) semi-insulating substrates available from Tamura Corporation of Japan were used for the growth studies. The substrates were synthesized by the EFG method. Pre-growth sample preparation involved solvent cleaning using acetone, toluene, and isopropyl alcohol followed by N_2 drying. Prior to the growth, the samples were in-situ annealed at 900 °C for 30 min under O_2 atmosphere. High purity gallium pellets (Alfa Aesar, 99.99999%) and oxygen (O_2) were used as the source materials, and argon (Ar) was used as the carrier gas. Silicon tetrachloride ($SiCl_4$) was used as the n-type dopant source. The growths were conducted at an oxygen volume percentage of ~4.8%. The growth pressure was set at ~4 Torr. The thin films were grown on 10 mm × 15 mm substrates, which is the maximum size commercially available.

The surface morphology, crystal quality, and electrical charge transport properties of the β-Ga_2O_3 homoepitaxial thin films were characterized by field emission scanning electron microscopy (FESEM), AFM, XRD rocking curve (RC), STEM, and temperature dependent Hall measurement. FESEM images were taken with a Helios 650. AFM images were taken with a Bruker AXS Dimension Icon. XRD RCs were collected on a Bruker D8 Discover. High angle annular dark field (HAADF) STEM images of the samples were acquired using a Thermo Fisher Scientific Titan scanning transmission electron microscope at 300 kV. The temperature dependent Hall measurement was carried out using two custom built systems. Below room temperature, an electromagnet with a vacuum cryostat with a closed-cycle He refrigerator was used. Above room temperature, an electromagnet with a quartz tube and a silicon carbide heater was used. Nitrogen gas was used to purge the quartz tube during high temperature measurements.

The surface morphology of the β-Ga_2O_3 homoepitaxial thin films was characterized by SEM and AFM. Figures 1(a) and 1(b) show the top view FESEM images of β-Ga_2O_3 (001) and (010) homoepitaxial thin films grown at 900 °C for 60 min. The surfaces of the thin films resembled a terrace like morphology and were composed of multi-step arrays. Figures 1(c) and 1(d) show the cross-sectional STEM images of the TEM samples obtained from the (001) and (010) homoepitaxial β-Ga_2O_3 thin films, respectively. The samples were prepared using the focused ion beam (FIB) lift-out method. Due to the homoepitaxial growth, the interfaces between the epi-layer and the substrate were not observable from the STEM images. Instead, the thicknesses of the homoepitaxial β-Ga2O3 thin films were estimated from secondary ion mass spectroscopy (SIMS). From the SIMS depth profiles (Fig. 5), the thicknesses of the (010 and (001) homoepitaxial layers were estimated to be ~1.9 μm and 1.2 μm which corresponded to growth rates of ~1.9 μm/h and ~1.2 μm/h, respectively. For comparison, recent reported

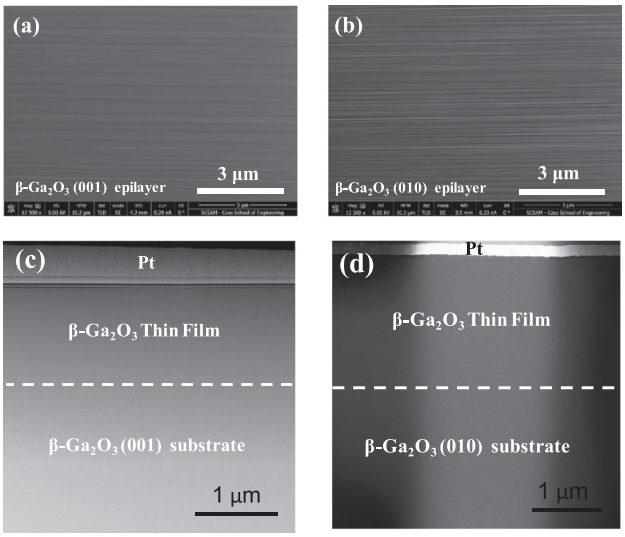

FIG. 1. Top view FESEM images of β-Ga_2O_3 (a) (001) and (b) (010) homoepitaxial thin films grown via LPCVD at 900 °C. (c) Low magnification HAADF STEM images of β-Ga_2O_3 (c) (001) and (d) (010) homoepitaxial thin films. The thin film thicknesses were estimated from SIMS depth profiles.

growth rates for β-Ga_2O_3 homoepitaxial thin films grown on β-Ga_2O_3 substrates were ~0.2 μm/h [MBE, (010) native substrate],[19] ~0.33 μm/h [MOVPE, (010) native substrate],[21] and ~5 μm/h [HVPE, (001) native substrate].[16] Figures 2(a) and 2(b) show the AFM images of the $5 \times 5\ \mu m^2$ scan for the homoepitaxial thin films surfaces. The RMS roughnesses for the (001) and (010) homoepitaxial thin films were ~3 nm and ~4 nm, respectively. The surface roughness did not show an obvious dependence on the Si doping level of the thin films. The roughness values were higher than the ones reported for the thin films grown by MBE[19] and MOVPE.[21] This was due to the much faster growth rate of the films grown by LPCVD compared to the ones grown by MBE or MOVPE. Note that

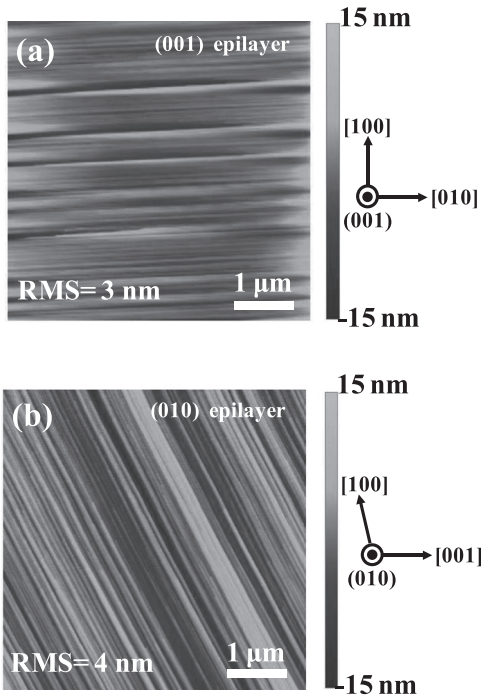

FIG. 2. Surface AFM images ($5\ \mu m \times 5\ \mu m$) of β-Ga_2O_3 (a) (001) and (b) (010) homoepitaxial thin films grown at 900 °C.

the reported HVPE grown films (growth rate ~5 μm/h) were composed of macrostep arrays with an average height of 280 nm.[16]

The crystal quality of the β-Ga_2O_3 homoepitaxial thin films was characterized by the XRD rocking curve measurement. Figure 3 shows the XRD rocking curves of the asymmetric (400) reflection peaks of β-Ga_2O_3 (001) and (-42-2) reflection peaks of β-Ga_2O_3 (010) homoepitaxial thin films and β-Ga_2O_3 substrates. No peaks associated with other phases (α, γ, δ, and ε) of Ga_2O_3 were detected in the 2 theta scan. This is a good indication that the films have grown homoepitaxially on the substrates and have only the β phase. While the full width at the half maximum (FWHM) of the (400) peak of the β-Ga_2O_3 (001) substrate was 27 arc sec, the FWHM value of the LPCVD grown Si doped thin film was 47 arc sec. The broadening of the FWHM indicates that the LPCVD grown thin film has slightly degraded crystal quality than the native substrate. The (-42-2) reflection peak of the β-Ga_2O_3 (010) homoepitaxial thin film [Fig. 3(b)] was taken at a grazing incidence angle of 1.3°. The penetration depth of this reflection was calculated to be <0.7 μm, indicating that the signal was primarily from the top film. The FWHM values of (-42-2) peaks for the (010) substrate and epi film were 77 and 83 arc sec, respectively. No shift of the XRD peak for the as-grown films relative to the substrates was observed for both cases, indicating that the thin films were free of strain. For comparison, the recent reported XRD rocking curve FWHMs of β-Ga_2O_3 homoepitaxial layers grown on (100) and (001) β-Ga_2O_3 substrates by MBE and HVPE are 72[14] and 60–78 arc sec,[16] respectively.

The crystalline quality of the β-Ga_2O_3 homoepitaxial thin films grown at 900 °C was further investigated with high magnification HAADF STEM images. Figures 4(a) and 4(b) show the STEM images of the (010) and (001) homoepitaxial thin films, respectively. High resolution images were acquired using non-rigid registration[24] of 30 fast-scanned images to increase the precision and signal to noise ratio. Along the [010] orientation [Fig. 4(a)], Ga atoms have the largest separation between them with an interatomic distance of ~3.3 Å.[25] On the other hand, the [001] orientation has a shorter distance between the columns [Fig. 4(b)]. No extended planar defects or dislocations were visible in the view fields of the STEM images for both thin films. However, point defects are expected to be present which resulted in lower carrier mobility than that predicted by theory as discussed later. Fundamentally, native point defects such as vacancies and interstitials of β-Ga_2O_3 thin films are expected to be complex due to their complicated monoclinic lattice with 2 Ga sites and 3O sites. Oxygen and gallium vacancies have been predicted to be deep donor and shallow acceptor based on density functional theory (DFT) calculation, respectively.[26] Korhonen *et al*. studied the vacancy defects in UID and Si-doped Ga_2O_3

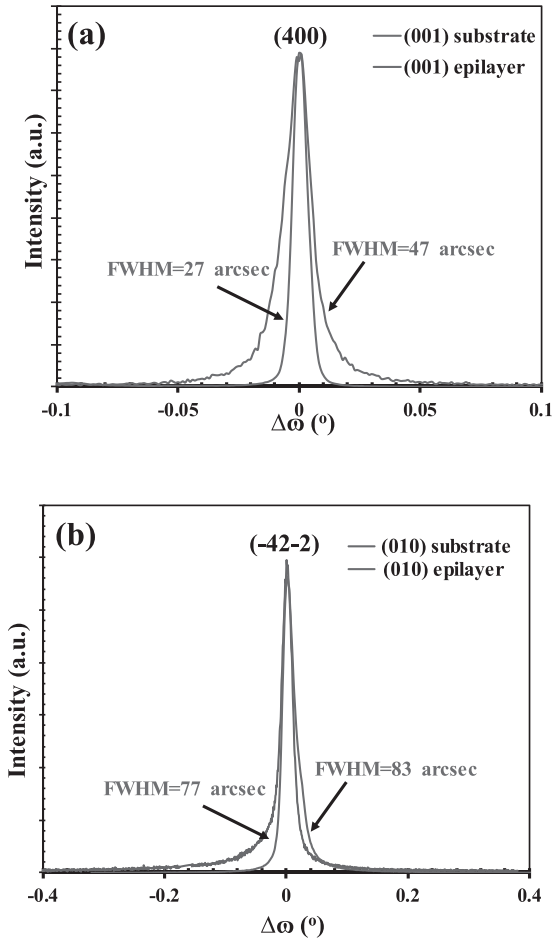

FIG. 3. XRD rocking curves of (a) (400) reflection peaks of β-Ga_2O_3 (001) and (b) (-42-2) reflection peaks of β-Ga_2O_3 (010) homoepitaxial thin films and β-Ga_2O_3 substrates.

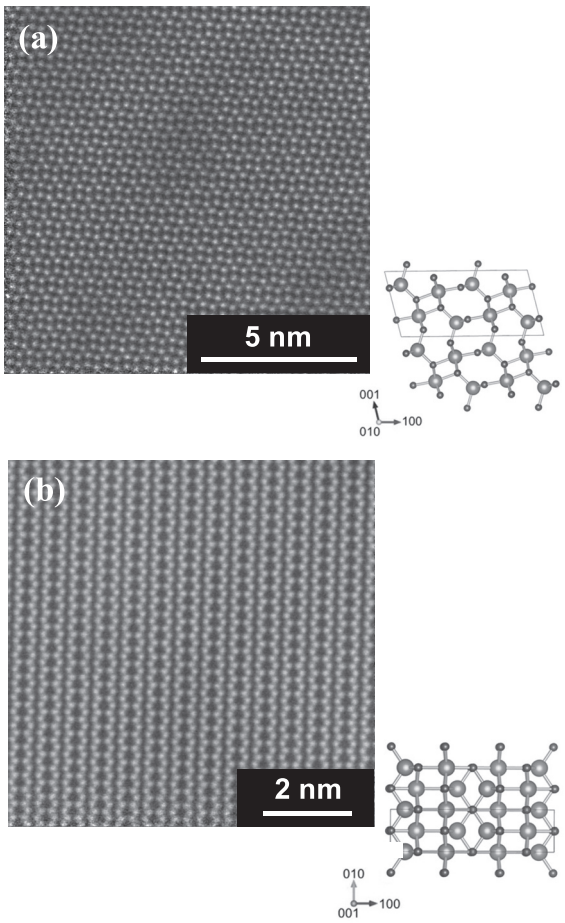

FIG. 4. High magnification HAADF STEM images of the (a) (010) and (b) (001) orientation view of the homoepitaxial thin films grown by LPCVD. Blue spheres represent Ga atoms, and red spheres represent oxygen atoms.

thin films grown by MOVPE using positron annihilation spectroscopy.[27]

Figure 5 shows the SIMS depth profiles of the impurity concentration for Si doped β-Ga_2O_3 homoepitaxial thin films grown at 900 °C on (001) and (010) β-Ga_2O_3 substrates. For both films, the Si doping profiles were mostly flat, indicating constant incorporation of the dopants throughout the growth process. A peak in the Si profile is visible at the interface between the epi-layer and the substrate for both films. The chemical Si concentrations in the (001) and (010) thin films measured by SIMS were 9.6×10^{17} cm^{-3} and 2.4×10^{18} cm^{-3}, respectively. The concentrations of other impurities in both thin films grown by LPCVD were comparable to those reported for HVPE grown films.[16]

To assist the understanding of the charge carrier transport properties of β-Ga_2O_3 grown along (010) and (001) substrates, temperature dependent Hall measurements were performed on the Si doped homoepitaxial thin films. Thin films with different doping levels were grown on each plane. By varying the doping source flow rate from 0.01 to 0.25 sccm, the carrier concentration was broadly tunable in the range between mid-10^{17} and low-10^{19} cm^{-3}. Figure 6 shows the temperature dependence of the n-type carrier concentration and the mobility of Si doped (001) and (010) homoepitaxial β-Ga_2O_3 thin films having room temperature carrier concentrations of 9.5×10^{17} cm^{-3} and 1.2×10^{18} cm^{-3}, respectively.

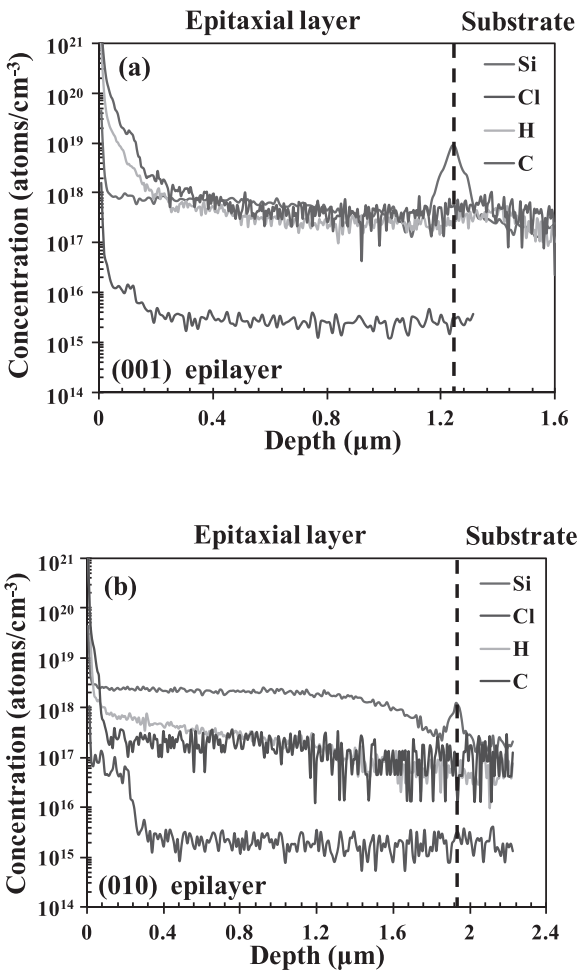

FIG. 5. SIMS depth profiles of impurities in the LPCVD grown Si-doped β-Ga_2O_3 homoepitaxial thin films on (a) (001) and (b) (010) β-Ga_2O_3 substrates.

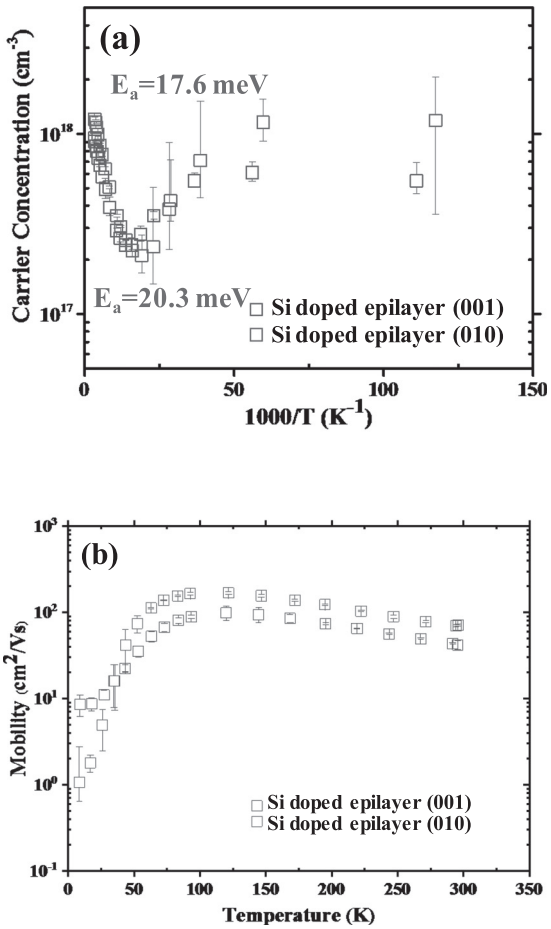

FIG. 6. Temperature dependent Hall measurement of (a) the carrier concentration and (b) mobility for the LPCVD grown Si-doped β-Ga_2O_3 homoepitaxial thin films on (001) and (010) β-Ga_2O_3 substrates.

The free carrier concentrations for both films were similar to the chemical Si concentrations measured by SIMS, indicating the effective incorporation of the dopants in the electrically active sites and negligible compensation. The thin films were grown under the same growth condition. The difference in the carrier concentration between the two films is due to the different Si incorporation rates along different orientations of β-Ga_2O_3. The activation energies of Si were estimated to be $E_a \sim 20.3$ meV and 17.6 meV ($n \sim e^{-Ea/kT}$) from the temperature dependence of the carrier concentration for the (001) and (010) thin films which were similar to the previously reported values.[28,29] For both films, the temperature dependence of the carrier concentration has a dip at ~70 K. Such phenomena have been observed previously from the Ge doped MBE grown homoepitaxial β-Ga_2O_3 thin films and the β-Ga_2O_3 bulk crystals grown by the floating zone method.[8,30] In a semiconductor material, the net conducting carrier concentration is composed of carriers from both donor and conduction bands.[31] The dominant contribution comes from the donor band at low temperatures and from the conduction band at high temperatures. The dip indicates the transition from the extrinsic region (donor band) to the intrinsic region (conduction band). Peak mobilities of ~100 cm^2/V s and ~170 cm^2/V s were obtained at ~120 K and ~122 K for the (001) and (010) homoepitaxial β-Ga_2O_3 thin films, respectively. The mobilities decreased to ~42 cm^2/V s and ~72 cm^2/V s at room temperature, respectively. The higher mobility from the

(010) film can be due to its lower point defect density. From Fig. 6(a), the carrier concentration did not change substantially at low temperatures for thin films of both orientations. Such a dependence of the carrier concentration and mobility on temperature for both films has been observed for Ge doped MBE grown homoepitaxial β-Ga_2O_3.[8] The electron mobility is also limited by ionized impurity scattering at low temperatures and optical phonon scattering at high temperatures.[32] For the Ge doped homoepitaxial (010) β-Ga_2O_3 with a room temperature carrier concentration of $\sim 6.1 \times 10^{17}$ cm^{-3} grown by MBE,[8] the peak mobility was $\sim 250\,cm^2/V$ s. At the similar carrier concentration, the room temperature Hall mobility of the LPCVD grown Si doped (010) homoepitaxial β-Ga_2O_3 thin film is comparable to the Ge ($80\,cm^2/V$ s at 2.8×10^{18} cm^{-3}) and Sn ($\sim 60\,cm^2/V$ s at $\sim 1.5 \times 10^{18}$ cm^{-3}) doped MBE grown thin films[18,19] and Si ($\sim 60\,cm^2/V$ s at $\sim 3 \times 10^{18}$ cm^{-3}) and Sn ($\sim 70\,cm^2/V$ s at $\sim 3 \times 10^{18}$ cm^{-3}) doped MOVPE grown thin films.[21] Note that the room temperature and low temperature Hall mobilities of all the thin films grown by MBE, MOVPE, and LPCVD so far are lower than the theoretically predicted values.[33] This can be related to the amount of native defects present in the thin films associated with each growth method, which is an ongoing research direction.

In summary, Si doped homoepitaxial (001) and (010) β-Ga_2O_3 thin films were grown on semi-insulating Fe doped β-Ga_2O_3 substrates via LPCVD. (001) and (010) homoepitaxial β-Ga_2O_3 thin films with RMS surface roughnesses of 3 and 4 nm and growth rates of $\sim 1.2\,\mu m/h$ and $\sim 1.9\,\mu m/h$ were obtained. The temperature dependence of the carrier concentration and mobility of the thin films were investigated using van der Pauw Hall pattern. Room temperature electron Hall mobilities of $\sim 72\,cm^2/V$ s and $\sim 42\,cm^2/V$ s were measured for Si doped homoepitaxial (010) and (001) β-Ga_2O_3 thin films with doping concentrations of $\sim 1.2 \times 10^{18}\,cm^{-3}$ and $\sim 9.5 \times 10^{17}\,cm^{-3}$ respectively. The growth of Si doped homoepitaxial (001) and (010) β-Ga_2O_3 thin films by LPCVD with high material quality, a relatively fast growth rate, and reasonable electron mobility opens up opportunities for vertical power devices with thick active layers.

The authors (Rafique, Karim, and Zhao) acknowledge the funding support from the National Science Foundation (DMR-1755479). The authors would like to thank Adam T. Neal and Shin Mou from Air Force Research Lab (AFRL) for their help on the temperature dependent Hall measurements for the β-Ga_2O_3 samples.

[1]S. Rafique, L. Han, and H. Zhao, Phys. Status Solidi A **213**, 1002 (2016).
[2]Y. Qu, Z. Wu, M. Ai, D. Guo, Y. An, H. Yang, L. Li, and W. Tang, J. Alloys Compd. **680**, 247 (2016).
[3]S. Rafique, L. Han, and H. Zhao, Phys. Status Solidi A **214**, 1700063 (2017).
[4]S. Nakagomi, T.-A. Sato, Y. Takahashi, and Y. Kokubun, Sens. Actuators, A **232**, 208 (2015).
[5]E. Ahmadi, Y. Oshima, F. Wu, and J. S. Speck, Semicond. Sci. Technol. **32**, 035004 (2017).
[6]E. Farzana, Z. Zhang, P. K. Paul, A. R. Arehart, and S. A. Ringel, Appl. Phys. Lett. **110**, 202102 (2017).
[7]K. Konishi, K. Goto, H. Murakami, Y. Kumagai, A. Kuramata, S. Yamakoshi, and M. Higashiwaki, Appl. Phys. Lett. **110**, 103506 (2017).
[8]N. Moser, J. Mccandless, A. Crespo, K. Leedy, A. Green, A. Neal, S. Mou, E. Ahmadi, J. S. Speck, K. Chabak, N. Peixoto, and G. Jessen, IEEE Electron. Dev. Lett. **38**, 775 (2017).
[9]S. Krishnamoorthy, Z. Xia, S. Bajaj, M. Brenner, and S. Rajan, Appl. Phys. Express **10**, 051102 (2017).
[10]M. H. Wong, Y. Nakata, A. Kuramata, S. Yamakoshi, and M. Higashiwaki, Appl. Phys. Express **10**, 041101 (2017).
[11]T. C. Lovejoy, E. N. Yitamben, N. Shamir, J. Morales, E. G. Villora, K. Shimamura, S. Zheng, F. S. Ohuchi, and M. A. Olmstead, Appl. Phys. Lett. **94**, 081906 (2009).
[12]M. Slomski, N. Blumenschein, P. P. Paskov, J. F. Muth, and T. Paskova, J. Appl. Phys. **121**, 235104 (2017).
[13]B. E. Kananen, L. E. Halliburton, K. T. Stevens, G. K. Foundos, and N. C. Giles, Appl. Phys. Lett. **110**, 202104 (2017).
[14]M.-Y. Tsai, O. Bierwagen, M. E. White, and J. S. Speck, J. Vac. Sci. Technol., A **28**, 354 (2010).
[15]G. Wagner, M. Baldini, D. Gogova, M. Schmidbauer, R. Schewski, M. Albrecht, Z. Galazka, D. Klimm, and R. Fornari, Phys. Status Solidi A **211**, 27 (2014).
[16]H. Murakami, K. Nomura, K. Goto, K. Sasaki, K. Kawara, Q. T. Thieu, R. Togashi, Y. Kumagai, M. Higashiwaki, A. Kuramata, S. Yamakoshi, B. Monemar, and A. Koukitu, Appl. Phys. Express **8**, 015503 (2015).
[17]S. Rafique, L. Han, M. J. Tadjer, J. A. Freitas, Jr., N. A. Mahadik, and H. Zhao, Appl. Phys. Lett. **108**, 182105 (2016).
[18]K. Sasaki, A. Kuramata, T. Masui, E. G. Villora, K. Shimamura, and S. Yamakoshi, Appl. Phys. Express **5**, 035502 (2012).
[19]E. Ahmadi, O. S. Koksaldi, S. W. Kaun, Y. Oshima, D. B. Short, U. K. Mishra, and J. S. Speck, Appl. Phys. Express **10**, 041102 (2017).
[20]M. Baldini, M. Albrecht, A. Fiedler, K. Irmscher, D. Klimm, R. Schewski, and G. Wagner, J. Mater. Sci. **51**, 3650 (2016).
[21]M. Baldini, M. Albrecht, A. Fiedler, K. Irmscher, R. Schewski, and G. Wagner, ECS J. Solid State Sci. Technol. **6**, Q3040 (2017).
[22]S. Rafique, L. Han, A. T. Neal, S. Mou, M. J. Tadjer, R. H. French, and H. Zhao, Appl. Phys. Lett. **109**, 132103 (2016).
[23]K. D. Leedy, K. D. Chabak, V. Vasilyev, D. C. Look, J. J. Boeckl, J. L. Brown, S. E. Tetlak, A. J. Green, N. A. Moser, A. Crespo, D. B. Thomson, R. C. Fitch, J. P. Mccandless, and G. H. Jessen, Appl. Phys. Lett. **111**, 012103 (2017).
[24]A. B. Yankovich, B. Berkels, W. Dahmen, P. Binev, S. I. Sanchez, S. A. Bradley, A. Li, I. Szlufarska, and P. M. Voyles, Nat. Commun. **5**, 4155 (2014).
[25]J. M. Johnson, S. Im, W. Windl, and J. Hwang, Ultramicroscopy **172**, 17 (2017).
[26]J. B. Varley, J. R. Weber, A. Janotti, C. G. Van, and D. Walle, Appl. Phys. Lett. **97**, 142106 (2010).
[27]E. Korhonen, F. Tuomisto, D. Gogova, G. Wagner, M. Baldini, Z. Galazka, R. Schewski, and M. Albrecht, Appl. Phys. Lett. **106**, 242103 (2015).
[28]A. Kuramata, K. Koshi, S. Watanabe, Y. Yamaoka, T. Masui, and S. Yamakoshi, Jpn. J. Appl. Phys., Part 1 **55**, 1202A2 (2016).
[29]M. R. Lorenz, J. F. Woods, and R. J. Gambino, J. Phys. Chem. Solids **28**, 403 (1967).
[30]E. G. Villora, K. Shimamura, T. Uijje, and K. Aoki, Appl. Phys. Lett. **92**, 202118 (2008).
[31]R. J. Molnar, T. Lei, and T. D. Moustakas, Appl. Phys. Lett. **62**, 72 (1993).
[32]M. J. Tadjer, N. A. Mahadik, V. D. Wheeler, E. R. Glaser, L. Ruppalt, A. D. Koehler, K. D. Hobart, C. R. Eddy, Jr., and F. J. Kub, ECS J. Solid State Sci. Technol. **5**, P468 (2016).
[33]N. Ma, N. Tanen, A. Verma, Z. Guo, T. Luo, H. Xing, and D. Jena, Appl. Phys. Lett. **109**, 212101 (2016).